

# UHKD: A Unified Framework for Heterogeneous Knowledge Distillation via Frequency-Domain Representations

Fengming Yu, Haiwei Pan, Kejia Zhang, Jian Guan, Haiying Jiang  
Department of Computer Science, Harbin Engineering University, Harbin, China  
{yufengming, panhaiwei, keji Zhang, j.guan, jianghaiying}@hrbeu.edu.cn

## Abstract

*Knowledge distillation (KD) is an effective model compression technique that transfers knowledge from a high-performance teacher to a lightweight student, reducing computational and storage costs while maintaining competitive accuracy. However, most existing KD methods are tailored for homogeneous models and perform poorly in heterogeneous settings, particularly when intermediate features are involved. Semantic discrepancies across architectures hinder effective use of intermediate representations from the teacher model, while prior heterogeneous KD studies mainly focus on the logits space, underutilizing rich semantic information in intermediate layers. To address this, Unified Heterogeneous Knowledge Distillation (UHKD) is proposed, a framework that leverages intermediate features in the frequency domain for cross-architecture transfer. Frequency-domain representations are leveraged to capture global semantic knowledge and mitigate representational discrepancies between heterogeneous teacher-student pairs. Specifically, a Feature Transformation Module (FTM) generates compact frequency-domain representations of teacher features, while a learnable Feature Alignment Module (FAM) projects student features and aligns them via multi-level matching. Training is guided by a joint objective combining mean squared error on intermediate features with Kullback-Leibler divergence on logits. Extensive experiments on CIFAR-100 and ImageNet-1K demonstrate the effectiveness of the proposed approach, achieving maximum gains of 5.59% and 0.83% over the latest heterogeneous distillation method on the two datasets, respectively. Code will be released soon.*

## 1. Introduction

Knowledge distillation (KD) has emerged as an effective technique for model compression and acceleration, aiming to reduce complexity while retaining as much performance as possible. This makes KD a practical solution for

deploying deep networks in resource-constrained environments. At the same time, the growing pursuit of accuracy has led to increasingly complex architectures such as CNNs [12, 28, 40], vision transformers (ViTs) [8, 27, 47], and MLPs [46, 48], whose heavy computational demands further highlight the need for compression.

KD was first introduced by Hinton et al.[15] as a technique in which a compact student is trained under the guidance of a larger, better-performing teacher. Besides ground-truth labels, the teacher provides soft targets as auxiliary supervision, helping the student approximate task objectives more effectively. This strategy reduces model size and cost, thereby improving inference efficiency while largely preserving accuracy. Existing approaches can be broadly categorized into three groups[10, 32]: (1) response-based methods, which transfer inter-class probability distributions via soft targets[15, 42, 52]; (2) feature-based methods, which distill intermediate representations to enhance representational capacity[14, 24, 39]; and (3) relation-based methods, which transfer structural knowledge among samples or features[35, 45, 53].

Although the above methods have achieved promising results in homogeneous distillation, in practice it is often difficult to obtain a high-performance teacher that shares the same architecture as the lightweight student. In homogeneous settings, intermediate features usually exhibit similar structural patterns, making direct alignment feasible. In contrast, heterogeneous models show substantial discrepancies in semantic abstraction and feature distribution, as shown in Fig. 1, which hinder effective use of intermediate features and lead to suboptimal results when homogeneous methods are directly applied. Recent studies on heterogeneous distillation typically focus on fixed transfer directions between specific architecture pairs, such as CNN to ViT or ViT to CNN[26, 30, 38, 47, 62–64]. While these works demonstrate feasibility, they often rely on complex, task-specific designs and remain limited to unidirectional transfer, lacking flexibility and generalization to arbitrary architecture pairs.

To overcome the limitations of unidirectional methods,

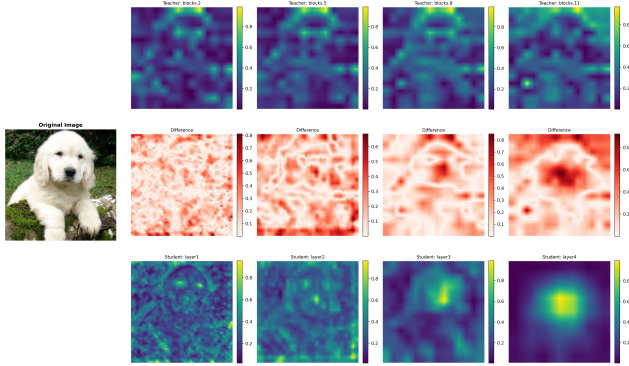


Figure 1. Intermediate feature visualization of different architectures. **Left:** original image. **Top right:** ViT-S (teacher) intermediate feature. **Bottom right:** ResNet-18 (student) intermediate feature. **Middle:** difference between teacher and student features.

recent studies have proposed more general heterogeneous distillation frameworks that handle arbitrary architecture combinations, such as OFA [11] and FBT [21]. OFA projects student intermediate representations into the logits space to bypass architectural discrepancies, while FBT employs weight sharing to construct auxiliary models that fuse heterogeneous architectures and generate additional supervision from logits and penultimate features. However, both approaches still rely on the logits space, offering only weak supervision and overlooking the rich structural and semantic knowledge in intermediate representations. Prior work has shown that neglecting such intermediate features reduces distillation effectiveness [54], indicating the need to explicitly leverage intermediate representations and address cross-architecture discrepancies for scalable and generalizable frameworks.

To address these issues, this paper proposes a **Unified Heterogeneous Knowledge Distillation (UHKD)** framework that exploits semantic information in intermediate representations through frequency-domain modeling. Frequency features aggregate spatial information and capture global semantic relationships [37], providing a principled bridge for knowledge transfer across heterogeneous architectures. Unlike prior fixed-architecture approaches, UHKD is general and applicable to arbitrary model combinations. It introduces two key components: a Feature Transformation Module (FTM), which performs spectral refinement and sequence transformation to obtain compact teacher representations, and a Feature Alignment Module (FAM), which employs a learnable adapter to project student features after FFT for better alignment. By aligning features in the frequency domain, UHKD alleviates semantic discrepancies and enables more effective knowledge transfer. The main contributions of this work are summarized as follows:

- UHKD is proposed, a frequency-based framework that

enables general and flexible knowledge transfer across arbitrary heterogeneous models by leveraging frequency-domain representations to bridge semantic gaps in intermediate features;

- Two key components, the FTM and the FAM, are designed, which together provide an effective mechanism for representing and aligning intermediate features in the frequency domain;
- Extensive experiments on CIFAR-100 and ImageNet-1K are conducted, and the results demonstrate that UHKD achieves favorable performance compared to existing baselines under diverse heterogeneous architecture combinations.

## 2. Related Work

### 2.1. Knowledge Distillation

Knowledge distillation is a widely used model compression technique that improves lightweight students by transferring knowledge from high-capacity teachers. Hinton et al.[15] first introduced KD via soft labels, followed by extensions such as response-based[9, 23, 42, 52, 59], feature-based[14, 20, 24, 39, 56], and relation-based methods[35, 36, 45, 50, 53].

Motivated by the success of Transformer architecture, heterogeneous KD has attracted increasing attention. Touvron et al.[47] introduced a distillation token for CNN to ViT transfer, while Ren et al.[38] extended this with multiple tokens to capture diverse inductive biases. Zhao et al.[62] decomposed CNN knowledge into local and global components, emphasizing local knowledge in early training to exploit inductive biases and introducing global knowledge later to enhance ViT learning. Liu et al.[26] pioneered ViT to CNN distillation by employing cross-attention to bridge and align heterogeneous feature representations. Other works tackled heterogeneous feature alignment by mapping features into unified receptive-field local representations [63], or by enabling collaborative learning among students with diverse inductive biases [30]. Recent frameworks such as OFA[11] and FBT[21] aim for generality by bridging feature gaps through logits or auxiliary models, improving flexibility but still limited in exploiting intermediate semantics.

### 2.2. Frequency-Domain Representations

Frequency-domain features have been widely applied in vision tasks such as classification[49, 51], object detection[17, 22, 43, 65], image generation[18], and super-resolution[33]. The amplitude spectrum encodes global attributes such as brightness and texture, while the phase spectrum preserves fine-grained structures like edges and orientations[31]. Leveraging these properties, Fourier-based methods have been shown to better capture long-

range dependencies and enhance texture consistency[44, 58, 67], leading to more discriminative representations. Recently, frequency-domain features have also been explored for KD[1, 37, 41, 60]. For instance, Pham et al.[37] emphasized that each frequency component aggregates information from the entire spatial domain, enabling better modeling of global semantics, while Zhang et al.[60] proposed suppressing harmful frequency components to alleviate information loss during downsampling.

While existing KD methods are mostly constrained to homogeneous settings, aligning intermediate semantics across heterogeneous models remains challenging. Frequency-domain features, with their strong global modeling capability, provide a promising direction for mitigating semantic discrepancies in heterogeneous architectures.

### 3. Method

#### 3.1. Overall Framework

This section introduces the Unified Heterogeneous Knowledge Distillation (UHKD) framework, as shown in Fig. 2. Direct alignment of intermediate features across heterogeneous architectures is hindered by large distributional gaps. UHKD addresses this challenge by transforming teacher and student features into a unified frequency space, which ensures consistency in both dimensionality and distribution. By leveraging semantic knowledge embedded in intermediate representations, UHKD enables flexible and effective knowledge transfer across diverse architectures.

#### 3.2. Feature Transformation Module

In heterogeneous KD, teacher intermediate features contain diverse semantic information, but their spatial distributions and structural forms differ significantly across architectures. To enable effective transfer, the FTM converts these features into a unified frequency-domain representation, facilitating subsequent alignment and distillation.

##### 3.2.1. Spectral Representation Refinement

The Fast Fourier Transform (FFT) is applied to convert teacher features from the spatial domain into the frequency domain. FFT is an efficient algorithm that reduces the complexity of the Discrete Fourier Transform [4] from  $\mathcal{O}(N^2)$  to  $\mathcal{O}(N \log N)$ . After transformation, only the magnitude spectrum is retained:

$$F_{FFT}^T = \|FFT(F^T)\|_2, \quad (1)$$

where  $F^T$  denotes teacher features. The magnitude encodes global structural information and energy distribution, while the phase mainly captures local details and positional cues [7, 31]. For heterogeneous KD, retaining only the magnitude yields stable, architecture-agnostic spectral representations while avoiding phase inconsistency that introduces bias across models.

To further refine these spectral features, a frequency filtering mechanism is applied after the FFT. The filter modulates components according to their distance from the spectrum center, with Gaussian decay ensuring smooth transitions and suppressing boundary artifacts. Two complementary masks are constructed: the low-frequency mask emphasizes central components to preserve global structure, while the high-frequency mask highlights distant components to retain edges and textures. The Gaussian-smoothed mask  $M$  is defined as:

$$M(f) = \exp\left(-\left(\frac{\|f - f_c\|}{\sigma}\right)^2\right), \quad (2)$$

where  $f$  and  $f_c$  denote the frequency coordinate and spectrum center, respectively, and  $\sigma$  is a bandwidth parameter controlling the emphasis on low-frequency or high-frequency regions. By combining the dual masks, the filter flexibly controls feature distributions across heterogeneous architectures, retaining critical information while suppressing redundant and boundary noise. The filtered teacher features are then obtained as:

$$F_{filter}^T = M \odot F_{FFT}^T. \quad (3)$$

##### 3.2.2. Sequence Representation Transformation

After spectral refinement, a parameter-free downsampling operation transforms teacher representations by removing redundancy and emphasizing dominant frequency components, while restructuring them into a unified sequence form  $(B, N, C)$  that standardizes feature dimensions across heterogeneous teacher models. Formally, the transformation is defined as:

$$F_{FTM}^T \in \mathbb{R}^{B \times N^T \times C^T} = \text{Reshape}(\text{AvgPool}(F_{filter}^T)), \quad (4)$$

where  $F_{FTM}^T$  denotes the output of the FTM, and  $N^T, C^T$  represent the sequence length and channel dimension of the teacher representations. This operation yields a compact, structured sequence that reduces computational overhead while preserving essential frequency components for effective heterogeneous knowledge transfer.

In summary, FTM enhances spectral features and restructures them into a unified and compact sequence representation, enabling efficient heterogeneous knowledge transfer.

#### 3.3. Feature Alignment Module

Based on the unified frequency-domain representations of the teacher model, the student features need to be adapted in both dimensionality and distribution. For this purpose, a learnable FAM is designed, which flexibly projects the intermediate features of the student model into a frequency-domain representation consistent with that of the teacher, thereby enabling efficient heterogeneous knowledge transfer.

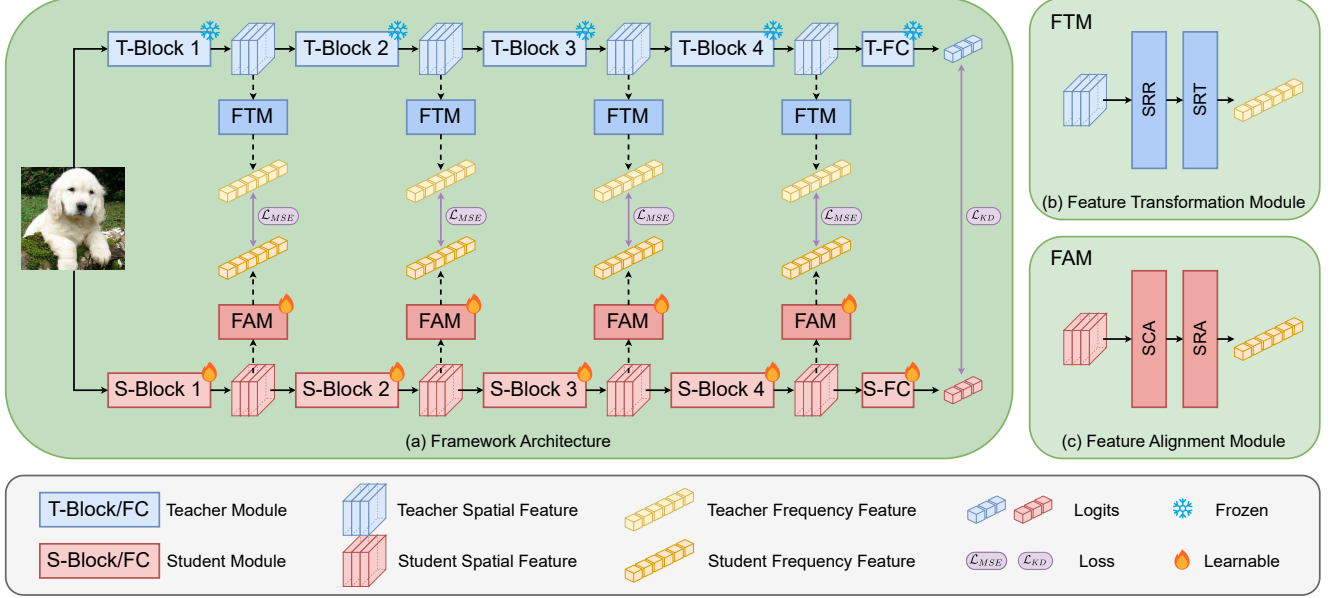


Figure 2. Overview of unified heterogeneous knowledge distillation. (a) The UHKD framework aligns teacher and student intermediate features in the frequency domain for effective knowledge transfer; (b) FTM module efficiently captures global representations of the teacher model through Spectral Representation Refinement (SRR) and Sequence Representation Transformation (SRT); (c) FAM module adapts student features through Spectral Channel Alignment (SCA) and Sequence Representation Alignment (SRA) to match the frequency-domain features of teacher model.

### 3.3.1. Spectral Channel Alignment

The student features are first transformed into the frequency domain via FFT, retaining only the magnitude spectrum as in FTM:

$$F_{FFT}^S = \|FFT(F^S)\|_2, \quad (5)$$

where  $F^S$  denotes the intermediate features of the student model. To address the dimensionality gap between student and teacher features in the spectral domain, a dimension-aware adaptive channel alignment mechanism is introduced. It projects the student channels from  $C^S$  to  $C^T$ , ensuring consistency with the teacher representation while preserving structural integrity. Formally, the aligned student features are obtained as:

$$F_{CA}^S = \text{ChannelAlign}_C(F_{FFT}^S), \quad (6)$$

where  $\text{ChannelAlign}_C$  denotes a learnable channel projection (linear mapping or  $1 \times 1$  convolution). This operation adjusts the channel dimensionality while maintaining spatial structure, enabling student features from diverse architectures to be efficiently aligned with teacher features.

### 3.3.2. Sequence Representation Alignment

To resolve the mismatch in sequence length between teacher and student features, a sequence representation alignment mechanism is applied after channel alignment. It reshapes the student features into a compact sequence representation and projects the length from  $N^S$  to  $N^T$ , ensuring consistency across heterogeneous architectures. Formally, the

aligned sequence features are obtained as:

$$F_{SA}^S \in \mathbb{R}^{B \times N^T \times C^T} = \text{SeqAlign}(F_{CA}^S). \quad (7)$$

These features are then normalized to match the distributional statistics of the teacher, yielding the final output:

$$F_{FAM}^S = \text{Norm}(F_{SA}^S), \quad (8)$$

In summary, FAM unifies heterogeneous feature representations in the frequency domain with learnable modules, yielding a compact and standardized sequence representation consistent with the teacher.

### 3.4. Distillation Formulation

With teacher features transformed by the FTM and student features adapted by the FAM, the heterogeneous intermediate representations are mapped into a unified frequency domain for effective alignment and knowledge transfer.

During training, a joint multi-loss strategy is adopted to enhance the student model. First, a mean squared error (MSE) loss constrains the consistency of frequency-domain feature distributions:

$$\mathcal{L}_{MSE} = \frac{1}{BN^T C^T} \|F_{FTM}^T - F_{FAM}^S\|_2^2. \quad (9)$$

Second, a Kullback-Leibler divergence loss aligns the output probability distributions of teacher and student, promoting class-level knowledge transfer:

$$\mathcal{L}_{KL} = D_{KL}(\text{softmax}(z^T/\tau) \parallel \text{softmax}(z^S/\tau)), \quad (10)$$

where  $z^T$  and  $z^S$  denote the logits of teacher and student, and  $\tau$  is the temperature factor. Finally, a cross-entropy loss  $\mathcal{L}_{CE}$  between student predictions and ground-truth labels preserves task-specific discriminative capability.

The three loss terms are combined in a weighted manner to guide student training:

$$\mathcal{L}_{total} = (1 - \lambda_{kl} - \lambda_{ce})\mathcal{L}_{MSE} + \lambda_{kl}\mathcal{L}_{KL} + \lambda_{ce}\mathcal{L}_{CE}, \quad (11)$$

where  $\lambda_{kl}$  and  $\lambda_{ce}$  are hyperparameters controlling the relative importance of each loss term. This joint optimization enables the student to learn from multiple perspectives, facilitating effective knowledge transfer and improved generalization in heterogeneous distillation.

## 4. Experiment

### 4.1. Experimental Setup

#### 4.1.1. Datasets

Experiments are conducted on two standard benchmarks, CIFAR-100 [19] and ImageNet-1K [6]. CIFAR-100 consists of 60,000 images of size  $32 \times 32$  across 100 classes, with 50,000 for training and 10,000 for testing, which poses a fine-grained recognition challenge due to its low resolution and large category set. ImageNet-1K contains 1.28 million training and 50,000 validation images in 1,000 classes, with images typically resized to  $224 \times 224$ , and serves as a standard large-scale benchmark for evaluating generalization and scalability.

#### 4.1.2. Models

Three representative categories of neural architectures are considered for evaluation. CNNs include ResNet [12], MobileNetV2 [40], and ConvNeXt [28]. Transformer-based models cover ViT [8], DeiT [47], Swin Transformer [27], and its lightweight variants Swin-Pico and Swin-Nano [11]. MLP-based models include MLP-Mixer [46] and ResMLP [48]. To enable consistent comparison across architectures, all models are uniformly divided into four stages for intermediate feature alignment, establishing a common structural granularity for heterogeneous distillation.

#### 4.1.3. Baselines

A comprehensive set of representative knowledge distillation methods is included for comparison. Feature-based approaches include FitNet [39], CC [36], RKD [35], and CRD [45], which focus on intermediate representations or relational knowledge. Response-based approaches include KD [15], DKD [61], and DIST [16], which align output distributions. Recent heterogeneous methods such as OFA [11] and FBT [21] are also considered. This selection covers both traditional homogeneous and recent heterogeneous approaches, ensuring a thorough comparison. Training details are reported in Appendix A.

## 4.2. Main Results

### 4.2.1. Results on CIFAR-100

Experiments are conducted on 12 heterogeneous teacher-student model pairs with different architectures on CIFAR-100, covering CNNs, ViTs, and MLPs. The detailed results are reported in Table 1.

Feature-based and response-based distillation methods perform poorly in heterogeneous settings. Feature-based approaches average only 69.72% top-1 accuracy, and direct alignment may even mislead the student, as in FitNet where ConvNeXt-T to Swin-P and ConvNeXt-T to ResMLP-S12 yield only 24.06% and 45.47%. Response-based methods perform slightly better with 72.79% on average, but still struggle. For instance, DIST collapses to 11.05% when distilling from Swin-T to ResMLP-S12 due to unreliable intra-class relation transfer under large feature discrepancies.

Heterogeneous methods such as OFA and FBT achieve competitive results but still make suboptimal use of intermediate representations. UHKD aligns teacher and student features in the frequency domain, bridging this gap and reaching 82.09% average top-1 accuracy, surpassing OFA and FBT by 4.45% and 2.25%. For example, MobileNetv2 students gain up to 5.58% over OFA (ViT-S to MobileNetv2), while ResMLP-S12 improves by 5.59% compared to FBT (ConvNeXt-T to ResMLP-S12). These results demonstrate the effectiveness of UHKD across diverse heterogeneous architectures over state-of-the-art baselines.

### 4.2.2. Results on ImageNet-1K

The proposed heterogeneous distillation method UHKD is further evaluated on ImageNet-1K dataset using 12 heterogeneous teacher-student model pairs, covering CNNs, ViTs, and MLPs. The detailed results are reported in Table 2.

Feature-based methods achieve 71.92% average top-1 accuracy, with the severe collapses seen on CIFAR-100 largely mitigated by the richer dataset and scale sensitivity of MLPs and Transformers [8, 34, 46]. Nevertheless, they still struggle with semantic gaps and may even degrade performance. For example, FitNet distillation from ConvNeXt-T to ResMLP-S12 achieves 74.69%, 1.96% lower than training from scratch. Response-based methods perform better, with an average accuracy of 73.38%, representing a 1.46% improvement over feature-based methods. DIST also benefits from the larger dataset, as the larger number of samples enables more reliable inter-class relation transfer.

Heterogeneous methods such as OFA and FBT achieve competitive results, with average top-1 accuracies of 73.96% and 74.26%, corresponding to gains of 0.58% and 0.88% over response-based methods. In comparison, the proposed UHKD leverages frequency-domain representations and the learnable alignment mechanism in FAM to achieve 74.64%, surpassing OFA and FBT by 0.68% and 0.38%, respectively. For instance, distillation from

Table 1. Top-1 accuracy (%) on CIFAR100. The best and second best results are in **bold** and underlined.

	Teacher	Student	From Scratch		Feature-based				Response-based			Heterogeneous-KD		
			T.	S.	FitNet	CC	RKD	CRD	KD	DKD	DIST	OFA	FBT	Ours
CNN-based students	Swin-T	ResNet18	89.26	74.01	78.87	74.19	74.11	77.63	78.74	80.26	77.75	80.54	<u>81.61</u>	<b>83.13</b>
	ViT-S	ResNet18	92.04	74.01	77.71	74.26	73.72	76.60	77.26	78.10	76.49	80.15	<u>81.93</u>	<b>83.60</b>
	Mixer-B/16	ResNet18	87.29	74.01	77.15	74.26	73.75	76.42	77.79	78.67	76.36	79.39	<u>81.90</u>	<b>82.98</b>
	Swin-T	MobileNetv2	89.26	73.68	74.28	71.19	69.00	79.80	74.68	71.07	72.89	80.98	<u>81.28</u>	<b>83.03</b>
	ViT-S	MobileNetv2	92.04	73.68	73.54	70.67	68.46	78.14	72.77	69.80	72.54	78.45	<u>82.10</u>	<b>84.03</b>
	Mixer-B/16	MobileNetv2	87.29	73.68	73.78	70.73	68.95	78.15	73.33	70.20	73.26	78.78	<u>80.83</u>	<b>83.67</b>
ViT-based students	ConvNeXt-T	DeiT-T	88.41	68.00	60.78	68.01	69.79	65.94	72.99	74.60	73.55	75.76	<b>79.57</b>	<u>77.03</u>
	Mixer-B/16	DeiT-T	87.29	68.00	71.05	68.13	69.89	65.35	71.36	73.44	71.67	73.90	<u>74.40</u>	<b>76.26</b>
	ConvNeXt-T	Swin-P	88.41	72.63	24.06	72.63	71.73	67.09	76.44	76.80	76.41	78.32	<u>80.73</u>	<b>83.26</b>
	Mixer-B/16	Swin-P	87.29	72.63	75.20	73.32	70.82	67.03	75.93	76.39	75.85	76.65	<u>78.44</u>	<b>81.72</b>
MLP-based students	ConvNeXt-T	ResMLP-S12	88.41	66.56	45.47	67.70	65.82	63.35	72.25	73.22	71.93	75.21	<u>78.03</u>	<b>83.62</b>
	Swin-T	ResMLP-S12	89.26	66.56	63.12	68.37	64.66	61.72	71.89	72.82	11.05	73.58	<u>77.20</u>	<b>82.72</b>
Average			88.85	71.45	66.25	71.12	70.06	71.44	74.62	74.61	69.15	77.64	<u>79.84</u>	<b>82.09</b>

Table 2. Top-1 accuracy (%) on ImageNet-1K. The best and second best results are in **bold** and underlined.

	Teacher	Student	From Scratch		Feature-based				Response-based			Heterogeneous-KD		
			T.	S.	FitNet	CC	RKD	CRD	KD	DKD	DIST	OFA	FBT	Ours
CNN-based students	DeiT-T	ResNet18	72.17	69.75	70.44	69.77	69.47	69.25	70.22	69.39	70.64	71.01	<u>71.22</u>	<b>71.42</b>
	Swin-T	ResNet18	81.38	69.75	71.18	70.07	68.89	69.09	71.14	71.10	70.91	71.76	<u>72.21</u>	<b>72.34</b>
	Mixer-B/16	ResNet18	76.62	69.75	70.78	70.05	69.46	68.40	70.89	69.89	70.66	71.38	<u>71.44</u>	<b>71.45</b>
	DeiT-T	MobileNetv2	72.17	68.87	70.95	70.69	69.72	69.60	70.87	70.14	71.08	71.39	<u>71.78</u>	<b>72.11</b>
	Swin-T	MobileNetv2	81.38	68.87	71.75	70.69	67.52	69.58	72.05	71.71	71.76	72.32	<u>72.54</u>	<b>72.80</b>
	Mixer-B/16	MobileNetv2	76.62	68.87	71.59	70.79	69.86	68.89	71.92	70.93	71.74	72.12	<u>72.31</u>	<b>72.89</b>
ViT-based students	ConvNeXt-T	DeiT-T	82.05	72.17	70.45	73.12	71.47	69.18	74.00	73.95	74.07	74.41	<u>75.26</u>	<b>76.09</b>
	Mixer-B/16	DeiT-T	76.62	72.17	74.38	72.82	72.24	68.23	74.16	72.82	74.22	74.46	<u>75.00</u>	<b>75.58</b>
	ConvNeXt-T	Swin-N	82.05	75.53	74.81	75.79	75.48	74.15	77.15	77.00	77.25	77.50	<u>77.73</u>	<b>77.84</b>
	Mixer-B/16	Swin-N	76.62	75.53	76.17	75.81	75.52	73.38	76.26	75.03	76.54	76.63	<u>76.87</u>	<b>77.26</b>
MLP-based students	ConvNeXt-T	ResMLP-S12	82.05	76.65	74.69	75.79	75.28	73.57	76.87	77.23	77.24	77.26	<u>77.33</u>	<b>78.05</b>
	Swin-T	ResMLP-S12	81.38	76.65	76.48	76.15	75.10	73.40	76.67	76.99	77.25	77.31	<u>77.42</u>	<b>77.90</b>
Average			78.43	72.05	72.81	72.63	71.67	70.56	73.51	73.02	73.61	73.96	<u>74.26</u>	<b>74.64</b>

ConvNeXt-T to DeiT-T yields 76.09% top-1 accuracy, exceeding OFA by 1.68% and FBT by 0.83%. Overall, these results demonstrate the robustness and scalability of UHKD across diverse architectures on large-scale datasets.

### 4.2.3. Results in Homogeneous Settings on ImageNet-1K

The proposed UHKD was evaluated on ImageNet-1K under homogeneous settings with two teacher-student pairs, ResNet34 to ResNet18 and ResNet50 to MobileNetV2. Both homogeneous-based [2, 3, 13, 16, 25, 45, 61] and heterogeneous-based [11, 21] methods were included for comparison. As shown in Table 3, UHKD achieves 72.71% and 73.52% on the two pairs, surpassing all baselines. These results indicate that the proposed UHKD is effective in both heterogeneous and homogeneous scenarios, confirming the robustness and general applicability.

## 4.3. Ablation Study

### 4.3.1. FFT in both FTM and FAM

The necessity of the FFT operation in both FTM and FAM is assessed by removing the FFT module and performing

feature alignment directly in the spatial domain. In this setting, teacher features are downsampled and aligned with student features through a learnable adapter. As reported in Table 4(a), the removal of FFT module consistently reduces the performance of student models on CIFAR-100. These results indicate that large architectural discrepancies between heterogeneous models cannot be effectively bridged in the spatial domain, even with a learnable adapter. In contrast, the global information captured in the frequency domain allows more effective alignment and leads to improved distillation performance.

### 4.3.2. Frequency Filter in FTM

The importance of the frequency filter in FTM is evaluated by removing it and transferring the full spectrum from teacher to student. As shown in Table 4(b), this leads to clear performance degradation because peripheral regions of the spectrum contain noise while most discriminative information lies near the center. Without filtering, noise is introduced and hampers student learning, whereas the filter suppresses redundant components and preserves dominant

Table 3. Top-1 accuracy (%) on ImageNet-1K for homogeneous model. The best and second best results are in **bold** and underlined.

Teacher	Student	From Scratch		Homo. Based							Hetero. Based		
		T.	S.	AT	OFD	CRD	Review	DKD	DIST	FCFD	OFA	FBT	Ours
ResNet34	ResNet18	73.31	69.75	70.69	70.81	71.17	71.61	71.70	72.07	72.24	72.10	<u>72.29</u>	<b>72.71</b>
ResNet50	MobileNetv2	79.86	68.87	69.56	71.25	71.37	72.56	72.05	73.24	73.37	73.28	<u>73.45</u>	<b>73.52</b>

information. The performance drop is even greater than that caused by removing the FFT, indicating that noisy components are amplified in the frequency domain and make the student model more vulnerable. These results highlight the critical role of frequency filtering in knowledge transfer.

Table 4. Ablation study on CIFAR-100: effect of the FFT module (w/o FFT) and frequency filter in FTM (w/o Freq F).

Teacher	Student	(a) w/o FFT	(b) w/o Freq F.	Ours
ConvNeXt-T	Swin-P	81.95 (-1.31)	81.90 (-1.36)	<b>83.26</b>
Mixer-B/16	DeiT-T	75.93 (-0.33)	75.69 (-0.57)	<b>76.26</b>
Swin-T	ResNet18	81.88 (-1.25)	81.58 (-1.55)	<b>83.13</b>
ConvNeXt-T	ResMLP-S12	82.24 (-1.38)	82.72 (-0.90)	<b>83.62</b>
ViT-S	MobileNetv2	82.24 (-1.52)	82.72 (-1.49)	<b>84.04</b>
Swin-T	MobileNetv2	80.69 (-2.34)	80.74 (-2.29)	<b>83.03</b>

### 4.3.3. Downsampling in FTM

The role of downsampling in FTM is examined by removing the downsampling module and directly aligning full-resolution frequency features. As shown in Table 5, this degrades performance across all evaluated teacher-student pairs. The results demonstrate the importance of downsampling, which reduces teacher feature resolution, enabling the student model to align more effectively, and aggregates local information while suppressing noise to support generalization, also reducing FAM parameter overhead.

Table 5. Ablation study on CIFAR-100: effect of DownSampling in FTM (w/o DownSampling).

Teacher	Student Pair	w/o DownSampling	Ours
Swin-T	ResNet18	82.04 (-1.09)	<b>83.13</b>
Swin-T	MobileNetv2	82.88 (-0.15)	<b>83.03</b>
Swin-T	ResMLP-S12	82.50 (-0.22)	<b>82.72</b>
ConvNeXt-T	Swin-P	81.32 (-1.94)	<b>83.26</b>
ConvNeXt-T	ResMLP-S12	83.58 (-0.04)	<b>83.62</b>

### 4.3.4. Learnable Module in FAM

The effectiveness of learnable parameters in FAM is assessed by comparison with non-parametric strategies, including bilinear interpolation (Bilinear), nearest-neighbor interpolation (Nearest), and a randomly initialized non-trainable variant (Random Init.). As shown in Table 6, all alternatives degrade performance, with interpolation in the ConvNeXt-T to Swin-P leading to an accuracy drop of over 16%. In contrast, the learnable FAM adds only a few parameters yet it more effectively adapts to feature discrepancies, achieving a favorable balance between parameter over-

head and accuracy. These results demonstrate the importance of learnable adaptation for robust feature alignment and knowledge transfer.

Table 6. Ablation study on CIFAR-100: effect of different alignment strategies in FAM.

Method	T: ViT-S S: ResNet18	T: ConvNeXt-T S: Swin-P	T: Swin-T S: ResMLP-S12
Bilinear	82.58 <sup>†</sup> (-1.02)	66.75 (-16.51)	79.91 (-2.81)
Nearest	82.55 (-1.05)	67.22 (-16.04)	77.85 (-4.87)
Random Init.	82.03 (-1.57)	78.92 (-4.34)	76.89 (-5.83)
<b>Ours</b>	<b>83.60</b>	<b>83.26</b>	<b>82.72</b>

<sup>†</sup> denotes linear interpolation for ViT-based teachers.

### 4.3.5. FTM/FAM Branch Counts and Layer Positions

The impact of the number and placement of distillation branches is examined on two teacher-student pairs with 1-4 branches, as reported in Table 7. Using only one branch significantly reduces performance regardless of its position. With two or three branches, deeper layers, especially the final one, provide greater benefits and narrow the gap with the default four-branch setting. Since deeper features capture global semantics and shallower ones provide complementary local details, combining branches across shallow, intermediate, and deep layers allows both types of information to be exploited, making the four-branch configuration the most effective.

Table 7. Ablation study on CIFAR-100: effect of different distillation branch counts and layer positions in FTM/FAM.

Stage	T: ConvNeXt-T S: Swin-P	T: ViT-S S: ResNet18
{1}	82.01 (-1.25)	83.10 (-0.50)
{2}	82.74 (-0.52)	83.05 (-0.55)
{3}	82.55 (-0.71)	82.79 (-0.81)
{4}	82.50 (-0.76)	83.03 (-0.57)
{1, 2}	83.19 (-0.07)	83.38 (-0.22)
{2, 3}	82.65 (-0.61)	82.93 (-0.67)
{3, 4}	82.96 (-0.30)	83.53 (-0.07)
{1, 2, 3}	83.02 (-0.24)	83.01 (-0.59)
{2, 3, 4}	83.20 (-0.06)	83.54 (-0.06)
{1, 2, 3, 4}	<b>83.26</b>	<b>83.60</b>

## 4.4. Discussion

To better understand the role of UHKD in mitigating heterogeneous representation discrepancy, a visual analysis is provided. As shown in Fig. 3(a), heterogeneous models (Swin-T and ResNet-18) exhibit substantial differences in

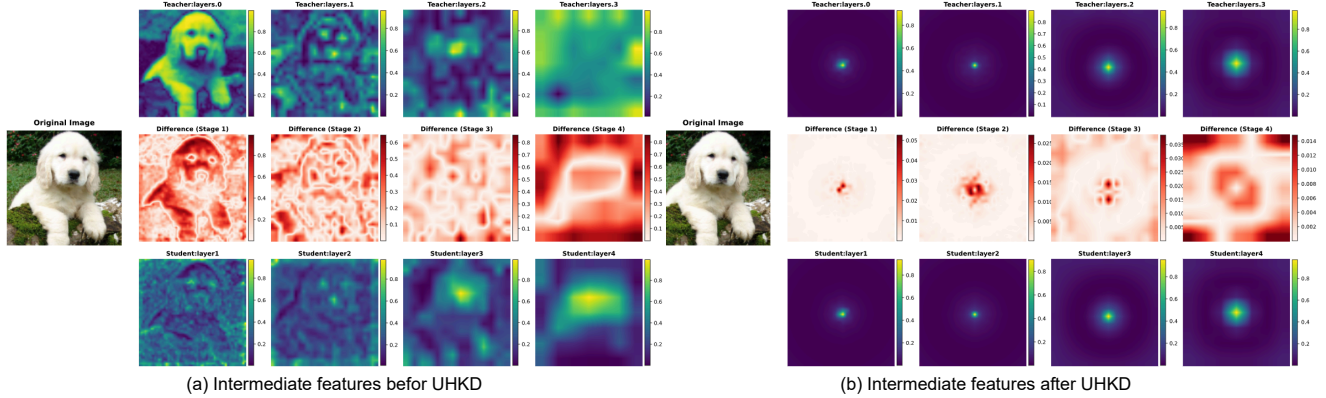


Figure 3. Visualization of intermediate features before and after UHKD. (a) Before UHKD; (b) After UHKD. In each case, the left column shows the original image, the top and bottom rows show feature maps from different stages of the Swin-T teacher and ResNet-18 student, and the middle row shows their difference maps.

Table 8. Comparison of parameter analysis between OFA and UHKD.

Teacher	Student	Teacher Para. (M)	Student Para. (M)	OFA					UHKD				
				Extra (M)	Trainable (M)	Extra Ratio (%)	Inference (M)	Comp. Ratio (%)	Extra (M)	Trainable (M)	Extra Ratio (%)	Inference (M)	Comp. Ratio (%)
DeiT-T	ResNet18	5.72	11.69	3.04	14.73	20.64	11.69	204.37	<b>2.01</b>	<b>13.70</b>	<b>14.67</b>	11.69	204.37
Swin-T	ResNet18	28.33	11.69	<b>4.39</b>	<b>16.08</b>	<b>27.30</b>	11.69	41.26	7.28	18.97	38.38	11.69	41.26
Mixer-B/16	ResNet18	59.88	11.69	4.39	16.08	27.30	11.69	19.52	<b>3.12</b>	<b>14.81</b>	<b>21.07</b>	11.69	19.52
DeiT-T	MobileNetV2	5.72	3.50	7.14	10.64	67.11	3.50	61.19	<b>1.83</b>	<b>5.33</b>	<b>34.33</b>	3.50	61.19
Swin-T	MobileNetV2	28.33	3.50	7.14	10.64	67.11	3.50	12.35	<b>6.82</b>	<b>10.32</b>	<b>66.09</b>	3.50	12.35
Mixer-B/16	MobileNetV2	59.88	3.50	7.14	10.64	67.11	3.50	5.85	<b>2.37</b>	<b>5.87</b>	<b>40.37</b>	3.50	5.85
ConvNeXt-T	DeiT-T	28.59	5.72	4.48	10.20	43.92	5.72	20.01	<b>1.28</b>	<b>7.00</b>	<b>18.29</b>	5.72	20.01
Mixer-B/16	DeiT-T	59.88	5.72	4.48	10.20	43.92	5.72	9.55	<b>1.50</b>	<b>7.22</b>	<b>20.78</b>	5.72	9.55
ConvNeXt-T	Swin-N	28.59	9.60	28.19	37.79	74.60	9.60	33.58	<b>6.36</b>	<b>15.96</b>	<b>39.85</b>	9.60	33.58
Mixer-B/16	Swin-N	59.88	9.60	28.19	37.79	74.60	9.60	16.03	<b>3.12</b>	<b>12.72</b>	<b>24.53</b>	9.60	16.03
ConvNeXt-T	ResMLP-S12	28.59	15.35	16.32	31.67	51.53	15.35	53.69	<b>1.59</b>	<b>16.94</b>	<b>9.39</b>	15.35	53.69
Swin-T	ResMLP-S12	28.33	15.35	16.32	31.67	51.53	15.35	54.18	<b>1.59</b>	<b>16.94</b>	<b>9.39</b>	15.35	54.18

feature structures and activation distributions, which hinder transfer under direct spatial matching. After applying FTM and FAM, the transformed features in Fig. 3(b) display a more compact spectral distribution with energy concentrated near the center, reducing structural discrepancies and indicating that the frequency domain serves as a normalization space for alignment across architectures. Additional statistical and visual analyses are reported in Appendix B.

A parameter analysis comparing UHKD with OFA is presented in Table 8, which reports the number of extra parameters (Extra), trainable parameters during distillation (Trainable), the proportion of extra parameters (Extra Ratio), inference parameters (Inference), and the compression ratio (Comp. Ratio). UHKD employs simple components for unified alignment across heterogeneous architectures and applies downsampling technology to teacher features, thereby avoiding complex adapters and reducing the parameter demand of the FAM. As a result, UHKD consistently requires fewer additional parameters than OFA. For instance, UHKD reduces extra parameters from 28.19M to 3.12M (74.60% to 24.53%) in Mixer-B/16 to Swin-N, and from 16.32M to 1.59M (51.53% to 9.39%) in ConvNeXt-T to ResMLP-S12. These reductions demonstrate that align-

ment and effective knowledge transfer can be achieved across diverse architectures with relatively low overhead.

## 5. Conclusion

In this paper, a unified heterogeneous knowledge distillation framework, **UHKD**, is proposed, introducing the frequency domain as a bridge for transferring intermediate representations across diverse architectures. Leveraging FFT, the FTM compacts and enhances teacher features, while the FAM adapts student features for robust cross-architecture alignment. In this way, UHKD overcomes the limitations of prior approaches that are restricted to homogeneous settings and rely mainly on logits-based supervision, leading to suboptimal use of intermediate semantic information.

Extensive experiments on CIFAR-100 and ImageNet-1K demonstrate that UHKD consistently outperforms existing methods across diverse models. These results highlight the effectiveness of frequency-domain representations in capturing global semantics and establish UHKD as a robust and unified framework for heterogeneous knowledge transfer, offering new insights into intermediate feature alignment and promoting model compression for efficient deployment.

## References

- [1] Le Minh Binh and Simon S. Woo. ADD: frequency attention and multi-view based knowledge distillation to detect low-quality compressed deepfake images. In *Thirty-Sixth AAAI Conference on Artificial Intelligence, AAAI 2022*, pages 122–130. AAAI Press, 2022. 3
- [2] Defang Chen, Jian-Ping Mei, Hailin Zhang, Can Wang, Yan Feng, and Chun Chen. Knowledge distillation with the reused teacher classifier. In *IEEE/CVF Conference on Computer Vision and Pattern Recognition, CVPR 2022*, pages 11923–11932. IEEE, 2022. 6
- [3] Pengguang Chen, Shu Liu, Hengshuang Zhao, and Jiaya Jia. Distilling knowledge via knowledge review. In *IEEE Conference on Computer Vision and Pattern Recognition, CVPR 2021*, pages 5008–5017. Computer Vision Foundation / IEEE, 2021. 6
- [4] James W Cooley and John W Tukey. An algorithm for the machine calculation of complex fourier series. *Mathematics of computation*, 19(90):297–301, 1965. 3
- [5] Ekin Dogus Cubuk, Barret Zoph, Jonathon Shlens, and Quoc Le. Randaugment: Practical automated data augmentation with a reduced search space. In *Advances in Neural Information Processing Systems 33: Annual Conference on Neural Information Processing Systems 2020, NeurIPS 2020*, 2020. 1
- [6] Jia Deng, Wei Dong, Richard Socher, Li-Jia Li, Kai Li, and Li Fei-Fei. Imagenet: A large-scale hierarchical image database. In *2009 IEEE conference on computer vision and pattern recognition*, pages 248–255. Ieee, 2009. 5
- [7] Xinghui Dong, Ying Gao, Junyu Dong, and Mike J. Chantler. The importance of phase to texture similarity. In *2017 IEEE International Conference on Computer Vision Workshops, ICCV Workshops 2017*, pages 2758–2766. IEEE Computer Society, 2017. 3
- [8] Alexey Dosovitskiy, Lucas Beyer, Alexander Kolesnikov, Dirk Weissenborn, Xiaohua Zhai, Thomas Unterthiner, Mostafa Dehghani, Matthias Minderer, Georg Heigold, Sylvain Gelly, Jakob Uszkoreit, and Neil Houlsby. An image is worth 16x16 words: Transformers for image recognition at scale. In *9th International Conference on Learning Representations, ICLR 2021*. OpenReview.net, 2021. 1, 5
- [9] Tommaso Furlanello, Zachary Chase Lipton, Michael Tschannen, Laurent Itti, and Anima Anandkumar. Born-again neural networks. In *Proceedings of the 35th International Conference on Machine Learning, ICML 2018*, pages 1602–1611. PMLR, 2018. 2
- [10] J. Gou, B. Yu, and S. J. Maybank. Knowledge distillation: A survey. *International Journal of Computer Vision*, 129(6): 1789–1819, 2021. 1
- [11] Zhiwei Hao, Jianyuan Guo, Kai Han, Yehui Tang, Han Hu, Yunhe Wang, and Chang Xu. One-for-all: Bridge the gap between heterogeneous architectures in knowledge distillation. In *Advances in Neural Information Processing Systems 36: Annual Conference on Neural Information Processing Systems 2023, NeurIPS 2023*, 2023. 2, 5, 6
- [12] Kaiming He, Xiangyu Zhang, Shaoqing Ren, and Jian Sun. Deep residual learning for image recognition. In *2016 IEEE Conference on Computer Vision and Pattern Recognition, CVPR 2016*, pages 770–778. IEEE Computer Society, 2016. 1, 5
- [13] Byeongho Heo, Jeessoo Kim, Sangdoo Yun, Hyojin Park, Nojun Kwak, and Jin Young Choi. A comprehensive overhaul of feature distillation. In *2019 IEEE/CVF International Conference on Computer Vision, ICCV 2019*, pages 1921–1930. IEEE, 2019. 6
- [14] Byeongho Heo, Minsik Lee, Sangdoo Yun, and Jin Young Choi. Knowledge transfer via distillation of activation boundaries formed by hidden neurons. In *The Thirty-Third AAAI Conference on Artificial Intelligence, AAAI 2019*, pages 3779–3787. AAAI Press, 2019. 1, 2
- [15] Geoffrey E. Hinton, Oriol Vinyals, and Jeffrey Dean. Distilling the knowledge in a neural network. *CoRR*, abs/1503.02531, 2015. 1, 2, 5
- [16] Tao Huang, Shan You, Fei Wang, Chen Qian, and Chang Xu. Knowledge distillation from A stronger teacher. In *Advances in Neural Information Processing Systems 35: Annual Conference on Neural Information Processing Systems 2022, NeurIPS 2022*, 2022. 5, 6
- [17] Zhipeng Huang, Zhizheng Zhang, Cuiling Lan, Zheng-Jun Zha, Yan Lu, and Baining Guo. Adaptive frequency filters as efficient global token mixers. In *IEEE/CVF International Conference on Computer Vision, ICCV 2023*, pages 6026–6036. IEEE, 2023. 2
- [18] Liming Jiang, Bo Dai, Wayne Wu, and Chen Change Loy. Focal frequency loss for image reconstruction and synthesis. In *2021 IEEE/CVF International Conference on Computer Vision, ICCV 2021*, pages 13899–13909. IEEE, 2021. 2
- [19] Alex Krizhevsky, Geoffrey Hinton, et al. Learning multiple layers of features from tiny images. 2009. 5
- [20] Shanshan Lao, Guanglu Song, Boxiao Liu, Yu Liu, and Yujia Yang. Masked autoencoders are stronger knowledge distillers. In *IEEE/CVF International Conference on Computer Vision, ICCV 2023*, pages 6361–6370. IEEE, 2023. 2
- [21] Guopeng Li, Qiang Wang, Ke Yan, Shouhong Ding, Yuan Gao, and Gui-Song Xia. Fuse before transfer: Knowledge fusion for heterogeneous distillation. In *Proceedings of the IEEE/CVF International Conference on Computer Vision*, pages 3445–3454, 2025. 2, 5, 6
- [22] Jian Li, Martin D. Levine, Xiangjing An, Xin Xu, and Hagen He. Visual saliency based on scale-space analysis in the frequency domain. *IEEE Trans. Pattern Anal. Mach. Intell.*, 35(4):996–1010, 2013. 2
- [23] Xuewei Li, Songyuan Li, Bourahla Omar, Fei Wu, and Xi Li. Reskd: Residual-guided knowledge distillation. *IEEE Transactions on Image Processing*, 30:4735–4746, 2021. 2
- [24] Sihao Lin, Hongwei Xie, Bing Wang, Kaicheng Yu, Xiaojun Chang, Xiaodan Liang, and Gang Wang. Knowledge distillation via the target-aware transformer. In *IEEE/CVF Conference on Computer Vision and Pattern Recognition, CVPR 2022*, pages 10905–10914. IEEE, 2022. 1, 2
- [25] Dongyang Liu, Meina Kan, Shiguang Shan, and Xilin Chen. Function-consistent feature distillation. In *The Eleventh International Conference on Learning Representations, ICLR 2023*. OpenReview.net, 2023. 6

- [26] Yufan Liu, Jiajiong Cao, Bing Li, Weiming Hu, Jingting Ding, and Liang Li. Cross-architecture knowledge distillation. In *Computer Vision - ACCV 2022*, pages 179–195. Springer, 2022. 1, 2
- [27] Ze Liu, Yutong Lin, Yue Cao, Han Hu, Yixuan Wei, Zheng Zhang, Stephen Lin, and Baining Guo. Swin transformer: Hierarchical vision transformer using shifted windows. In *2021 IEEE/CVF International Conference on Computer Vision, ICCV 2021*, pages 9992–10002. IEEE, 2021. 1, 5
- [28] Zhuang Liu, Hanzi Mao, Chao-Yuan Wu, Christoph Feichtenhofer, Trevor Darrell, and Saining Xie. A convnet for the 2020s. In *IEEE/CVF Conference on Computer Vision and Pattern Recognition, CVPR 2022*, pages 11966–11976. IEEE, 2022. 1, 5
- [29] Ilya Loshchilov and Frank Hutter. Decoupled weight decay regularization. In *7th International Conference on Learning Representations, ICLR 2019*. OpenReview.net, 2019. 1
- [30] Jianyuan Ni, Hao Tang, Yuzhang Shang, Bin Duan, and Yan Yan. Adaptive cross-architecture mutual knowledge distillation. In *18th IEEE International Conference on Automatic Face and Gesture Recognition, FG 2024*, pages 1–5. IEEE, 2024. 1, 2
- [31] A.V. Oppenheim and J.S. Lim. The importance of phase in signals. *Proceedings of the IEEE*, 69(5):529–541, 1981. 2, 3
- [32] Haiwei Pan, Fengming Yu, Kejia Zhang, Haiyan Lan, Qingyu Meng, and Zhe Li. Knowledge distillation in visual algorithms: A survey. *Journal of Computer Research and Development*, 62:1–33, 2025. 1
- [33] Yingxue Pang, Xin Li, Xin Jin, Yaojun Wu, Jianzhao Liu, Sen Liu, and Zhibo Chen. FAN: frequency aggregation network for real image super-resolution. In *Computer Vision - ECCV 2020 Workshops*, pages 468–483. Springer, 2020. 2
- [34] Namuk Park and Songkuk Kim. How do vision transformers work? In *The Tenth International Conference on Learning Representations, ICLR 2022*. OpenReview.net, 2022. 5
- [35] Wonpyo Park, Dongju Kim, Yan Lu, and Minsu Cho. Relational knowledge distillation. In *IEEE Conference on Computer Vision and Pattern Recognition, CVPR 2019*, pages 3967–3976. Computer Vision Foundation / IEEE, 2019. 1, 2, 5
- [36] Baoyun Peng, Xiao Jin, Dongsheng Li, Shunfeng Zhou, Yichao Wu, Jiaheng Liu, Zhaoning Zhang, and Yu Liu. Correlation congruence for knowledge distillation. In *2019 IEEE/CVF International Conference on Computer Vision, ICCV 2019*, pages 5006–5015. IEEE, 2019. 2, 5
- [37] Cuong Pham, Van-Anh Nguyen, Trung Le, Dinh Q. Phung, Gustavo Carneiro, and Thanh-Toan Do. Frequency attention for knowledge distillation. In *IEEE/CVF Winter Conference on Applications of Computer Vision, WACV 2024*, pages 2266–2275. IEEE, 2024. 2, 3
- [38] Sucheng Ren, Zhengqi Gao, Tianyu Hua, Zihui Xue, Yonglong Tian, Shengfeng He, and Hang Zhao. Co-advise: Cross inductive bias distillation. In *IEEE/CVF Conference on Computer Vision and Pattern Recognition, CVPR 2022*, pages 16752–16761. IEEE, 2022. 1, 2
- [39] Adriana Romero, Nicolas Ballas, Samira Ebrahimi Kahou, Antoine Chassang, Carlo Gatta, and Yoshua Bengio. Fitnets: Hints for thin deep nets. In *3rd International Conference on Learning Representations, ICLR 2015*, 2015. 1, 2, 5
- [40] Mark Sandler, Andrew G. Howard, Menglong Zhu, Andrey Zhmoginov, and Liang-Chieh Chen. Mobilenetv2: Inverted residuals and linear bottlenecks. In *2018 IEEE Conference on Computer Vision and Pattern Recognition, CVPR 2018*, pages 4510–4520. Computer Vision Foundation / IEEE Computer Society, 2018. 1, 5
- [41] Sungho Shin, Joosoon Lee, Junseok Lee, Yeonguk Yu, and Kyoobin Lee. Teaching where to look: Attention similarity knowledge distillation for low resolution face recognition. In *Computer Vision - ECCV 2022*, pages 631–647. Springer, 2022. 3
- [42] Wonchul Son, Jaemin Na, Junyong Choi, and Wonjun Hwang. Densely guided knowledge distillation using multiple teacher assistants. In *2021 IEEE/CVF International Conference on Computer Vision, ICCV 2021*, pages 9375–9384. IEEE, 2021. 1, 2
- [43] Yanguang Sun, Chunyan Xu, Jian Yang, Hanyu Xuan, and Lei Luo. Frequency-spatial entanglement learning for camouflaged object detection. In *Computer Vision - ECCV 2024*, pages 343–360. Springer, 2024. 2
- [44] Matthew Tancik, Pratul P. Srinivasan, Ben Mildenhall, Sara Fridovich-Keil, Nithin Raghavan, Utkarsh Singhal, Ravi Ramamoorthi, Jonathan T. Barron, and Ren Ng. Fourier features let networks learn high frequency functions in low dimensional domains. In *Advances in Neural Information Processing Systems 33: Annual Conference on Neural Information Processing Systems 2020, NeurIPS 2020*, 2020. 3
- [45] Yonglong Tian, Dilip Krishnan, and Phillip Isola. Contrastive representation distillation. In *8th International Conference on Learning Representations, ICLR 2020*. OpenReview.net, 2020. 1, 2, 5, 6
- [46] Ilya O. Tolstikhin, Neil Houlsby, Alexander Kolesnikov, Lucas Beyer, Xiaohua Zhai, Thomas Unterthiner, Jessica Yung, Andreas Steiner, Daniel Keysers, Jakob Uszkoreit, Mario Lucic, and Alexey Dosovitskiy. Mlp-mixer: An all-mlp architecture for vision. In *Advances in Neural Information Processing Systems 34: Annual Conference on Neural Information Processing Systems 2021, NeurIPS 2021*, pages 24261–24272, 2021. 1, 5
- [47] Hugo Touvron, Matthieu Cord, Matthijs Douze, Francisco Massa, Alexandre Sablayrolles, and Hervé Jégou. Training data-efficient image transformers & distillation through attention. In *Proceedings of the 38th International Conference on Machine Learning, ICML 2021*, pages 10347–10357. PMLR, 2021. 1, 2, 5
- [48] Hugo Touvron, Piotr Bojanowski, Mathilde Caron, Matthieu Cord, Alaaeldin El-Nouby, Edouard Grave, Gautier Izacard, Armand Joulin, Gabriel Synnaeve, Jakob Verbeek, and Hervé Jégou. Resmlp: Feedforward networks for image classification with data-efficient training. *IEEE Trans. Pattern Anal. Mach. Intell.*, 45(4):5314–5321, 2023. 1, 5
- [49] Travis L. Williams and Robert Li. Wavelet pooling for convolutional neural networks. In *6th International Conference on Learning Representations, ICLR 2018*. OpenReview.net, 2018. 2

- [50] Haohang Xu, Jiemin Fang, Xiaopeng Zhang, Lingxi Xie, Xinggang Wang, Wenrui Dai, Hongkai Xiong, and Qi Tian. Bag of instances aggregation boosts self-supervised distillation. In *The Tenth International Conference on Learning Representations, ICLR 2022*. OpenReview.net, 2022. 2
- [51] Kai Xu, Minghai Qin, Fei Sun, Yuhao Wang, Yen-Kuang Chen, and Fengbo Ren. Learning in the frequency domain. In *2020 IEEE/CVF Conference on Computer Vision and Pattern Recognition, CVPR 2020*, pages 1737–1746. Computer Vision Foundation / IEEE, 2020. 2
- [52] Chenglin Yang, Lingxi Xie, Siyuan Qiao, and Alan L. Yuille. Training deep neural networks in generations: A more tolerant teacher educates better students. In *The Thirty-Third AAAI Conference on Artificial Intelligence, AAAI 2019*, pages 5628–5635. AAAI Press, 2019. 1, 2
- [53] Junho Yim, Donggyu Joo, Ji-Hoon Bae, and Junmo Kim. A gift from knowledge distillation: Fast optimization, network minimization and transfer learning. In *2017 IEEE Conference on Computer Vision and Pattern Recognition, CVPR 2017*, pages 7130–7138. IEEE Computer Society, 2017. 1, 2
- [54] Zony Yu, Yuqiao Wen, and Lili Mou. Revisiting intermediate-layer matching in knowledge distillation: Layer-selection strategy doesn’t matter (much). *arXiv preprint arXiv:2502.04499*, 2025. 2
- [55] Sangdoon Yun, Dongyoon Han, Sanghyuk Chun, Seong Joon Oh, Youngjoon Yoo, and Junsuk Choe. Cutmix: Regularization strategy to train strong classifiers with localizable features. In *2019 IEEE/CVF International Conference on Computer Vision, ICCV 2019*, pages 6022–6031. IEEE, 2019. 1
- [56] Sergey Zagoruyko and Nikos Komodakis. Paying more attention to attention: Improving the performance of convolutional neural networks via attention transfer. In *5th International Conference on Learning Representations, ICLR 2017*. OpenReview.net, 2017. 2
- [57] Hongyi Zhang, Moustapha Cissé, Yann N. Dauphin, and David Lopez-Paz. mixup: Beyond empirical risk minimization. In *6th International Conference on Learning Representations, ICLR 2018*. OpenReview.net, 2018. 1
- [58] Juntao Zhang, Kun Bian, Peng Cheng, Wenbo An, Jianing Liu, and Jun Zhou. Vim-f: Visual state space model benefiting from learning in the frequency domain. *CoRR*, abs/2405.18679, 2024. 3
- [59] Ying Zhang, Tao Xiang, Timothy M. Hospedales, and Huchuan Lu. Deep mutual learning. In *2018 IEEE Conference on Computer Vision and Pattern Recognition, CVPR 2018*, pages 4320–4328. Computer Vision Foundation / IEEE Computer Society, 2018. 2
- [60] Yuan Zhang, Tao Huang, Jiaming Liu, Tao Jiang, Kuan Cheng, and Shanghang Zhang. Freekd: Knowledge distillation via semantic frequency prompt. In *IEEE/CVF Conference on Computer Vision and Pattern Recognition, CVPR 2024*, pages 15931–15940. IEEE, 2024. 3
- [61] Borui Zhao, Quan Cui, Renjie Song, Yiyu Qiu, and Jiajun Liang. Decoupled knowledge distillation. In *IEEE/CVF Conference on Computer Vision and Pattern Recognition, CVPR 2022*, pages 11943–11952. IEEE, 2022. 5, 6
- [62] Borui Zhao, Renjie Song, and Jiajun Liang. Cumulative spatial knowledge distillation for vision transformers. In *IEEE/CVF International Conference on Computer Vision, ICCV 2023*, pages 6123–6132. IEEE, 2023. 1, 2
- [63] Weisong Zhao, Xiangyu Zhu, Zhixiang He, Xiaoyu Zhang, and Zhen Lei. Cross-architecture distillation for face recognition. In *Proceedings of the 31st ACM International Conference on Multimedia, MM 2023*, pages 8076–8085. ACM, 2023. 2
- [64] Zhimeng Zheng, Tao Huang, Gongsheng Li, and Zuyi Wang. Promoting cnns with cross-architecture knowledge distillation for efficient monocular depth estimation. *CoRR*, abs/2404.16386, 2024. 1
- [65] Yijie Zhong, Bo Li, Lv Tang, Senyun Kuang, Shuang Wu, and Shouhong Ding. Detecting camouflaged object in frequency domain. In *IEEE/CVF Conference on Computer Vision and Pattern Recognition, CVPR 2022*, pages 4494–4503. IEEE, 2022. 2
- [66] Zhun Zhong, Liang Zheng, Guoliang Kang, Shaozi Li, and Yi Yang. Random erasing data augmentation. In *The Thirty-Fourth AAAI Conference on Artificial Intelligence, AAAI 2020*, pages 13001–13008. AAAI Press, 2020. 1
- [67] Man Zhou, Hu Yu, Jie Huang, Feng Zhao, Jinwei Gu, Chen Change Loy, Deyu Meng, and Chongyi Li. Deep fourier up-sampling. In *Advances in Neural Information Processing Systems 35: Annual Conference on Neural Information Processing Systems 2022, NeurIPS 2022*, 2022. 3

# UHKD: A Unified Framework for Heterogeneous Knowledge Distillation via Frequency-Domain Representations

## Supplementary Material

### A. Training Details

All models are trained using the AdamW[29] optimizer with momentum parameters ( $\beta_1 = 0.9$ ,  $\beta_2 = 0.999$ ), a weight decay of 0.005, and a numerical stability constant  $\epsilon = 1 \times 10^{-8}$ . A cosine learning rate schedule with warm-up is adopted to facilitate stable convergence. To further regularize training, label smoothing with a factor of 0.1 is applied and gradient clipping with a maximum norm of 5.0 is employed to prevent exploding gradients. For data augmentation, a strong strategy is used that combines RandAugment[5], Mixup[57], CutMix[55], and random erasing[66], in addition to standard techniques such as color jittering, random cropping, and horizontal flipping. The total loss follows the formulation in Eq. 11, where  $\lambda_{kl} = 0.4$  and  $\lambda_{ce} = 0.3$ , resulting in relative weights of 0.3, 0.4, and 0.3 for the mean squared error, Kullback-Leibler divergence, and cross-entropy terms, respectively. For feature-level distillation, four alignment points are selected uniformly along the network depth to capture shallow, middle, and deep stages of representation learning. All experiments are trained until convergence under carefully controlled settings, where optimization and augmentation strategies follow the same overall design.

### B. Supplementary Analyses of UHKD

To further illustrate the effectiveness of UHKD, additional visualization and statistical analyses are provided. Cosine similarity and Pearson correlation coefficients are calculated between teacher and student feature maps at different stages, as shown in Fig. 4. Before UHKD, cosine similarities remain consistently low, with values close to zero in the deep stage, indicating a pronounced representational gap. After the application of FTM and FAM, similarities increase significantly across all stages, with the most notable improvements observed in deeper layers where semantic abstraction is more prominent. A comparable trend is observed in the Pearson correlation analysis. The coefficients are close to zero before transformation, reflecting uncorrelated feature structures, but rise toward the upper bound after UHKD processing, signifying strong correspondence and structural coherence between teacher and student representations.

Building upon these observations, supplementary analyses are conducted on additional teacher-student pairs. The similarity results, as illustrated in Fig. 5, 8, and 9, show that both cosine similarity and Pearson correlation remain

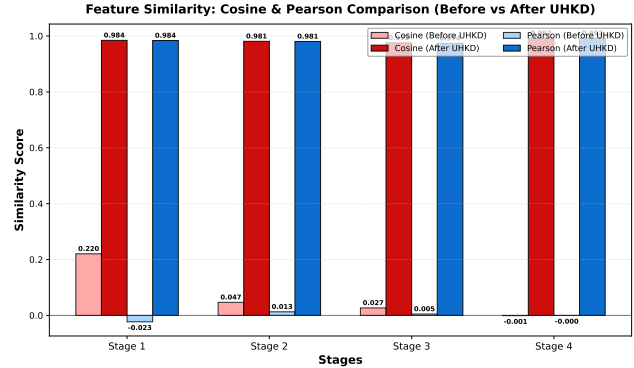


Figure 4. Comparison of feature similarities before and after UHKD between Swin-T and ResNet-18. Red bars denote cosine similarity, and blue bars denote Pearson correlation.

low before UHKD, particularly in deeper layers, reflecting substantial representational gaps. After the application of FTM and FAM, significant improvements are observed across all stages. The corresponding visualizations reveal more compact spectral distributions and reduced structural discrepancies, supporting the statistical findings, as shown in Fig. 6, 7, and 10. In Fig. 10, the sequence features of the Mixer-B/16 teacher are converted into feature maps for visualization, and this conversion results in intermediate layers where the energy concentration is not located at the center. This phenomenon reflects the structural characteristics of the teacher model rather than a limitation of UHKD.

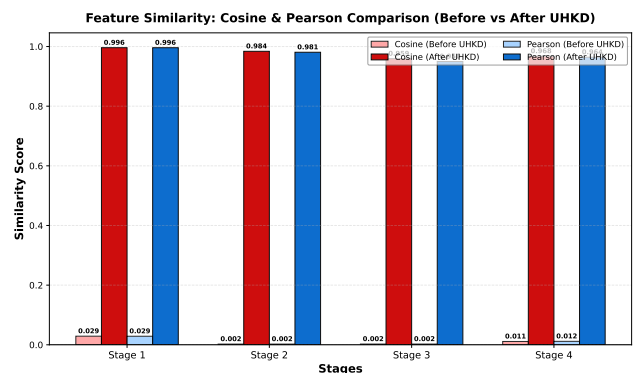


Figure 5. Comparison of feature similarities before and after UHKD between Swin-T and ResMLP-S12. Red bars denote cosine similarity, and blue bars denote Pearson correlation.

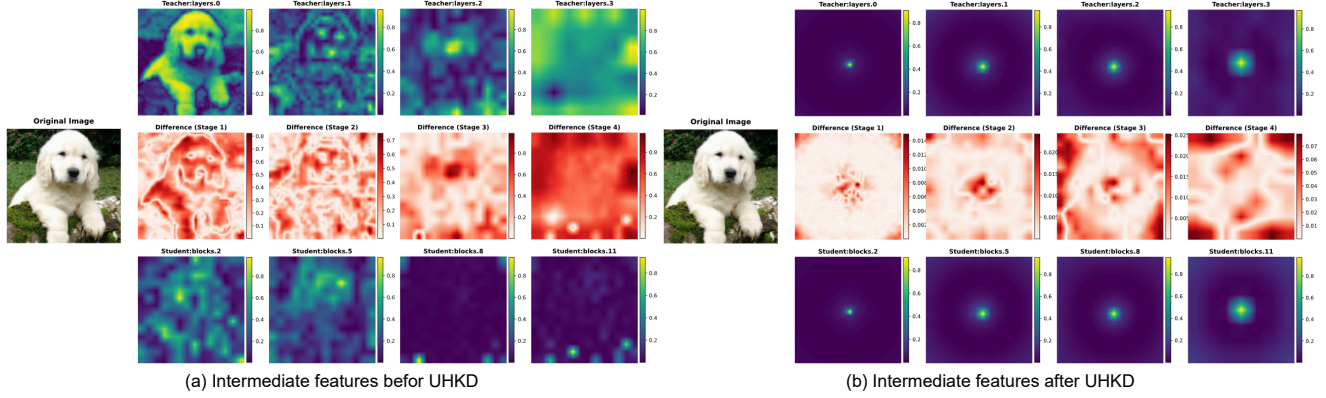


Figure 6. Visualization of intermediate features before and after UHKD. (a) Before UHKD; (b) After UHKD. In each case, the left column shows the original image, the top and bottom rows show feature maps from different stages of the Swin-T teacher and ResMLP-S12 student, and the middle row shows their difference maps.

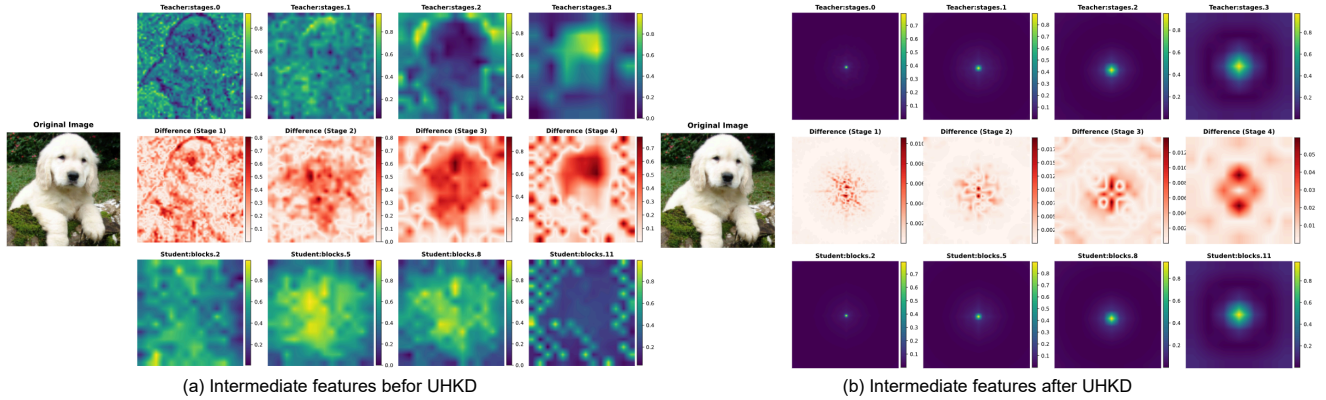


Figure 7. Visualization of intermediate features before and after UHKD. (a) Before UHKD; (b) After UHKD. In each case, the left column shows the original image, the top and bottom rows show feature maps from different stages of the ConvNeXt-T teacher and DeiT-T student, and the middle row shows their difference maps.

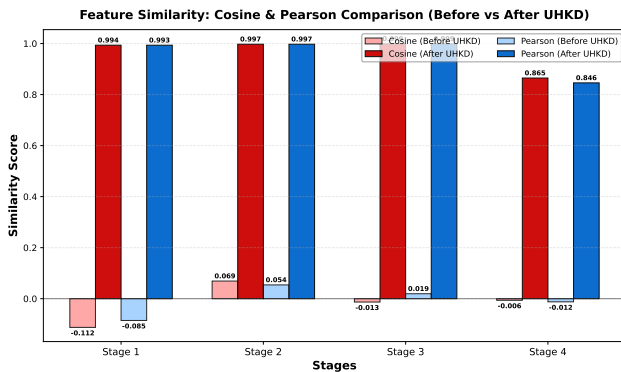


Figure 8. Comparison of feature similarities before and after UHKD between ConvNeXt-T and DeiT-T. Red bars denote cosine similarity, and blue bars denote Pearson correlation.

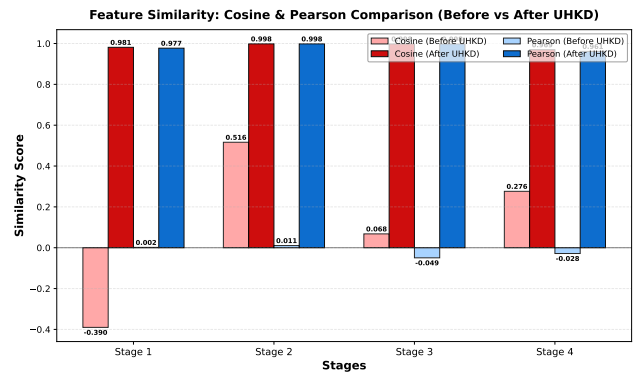


Figure 9. Comparison of feature similarities before and after UHKD between Mixer-B/16 and Swin-N. Red bars denote cosine similarity, and blue bars denote Pearson correlation.

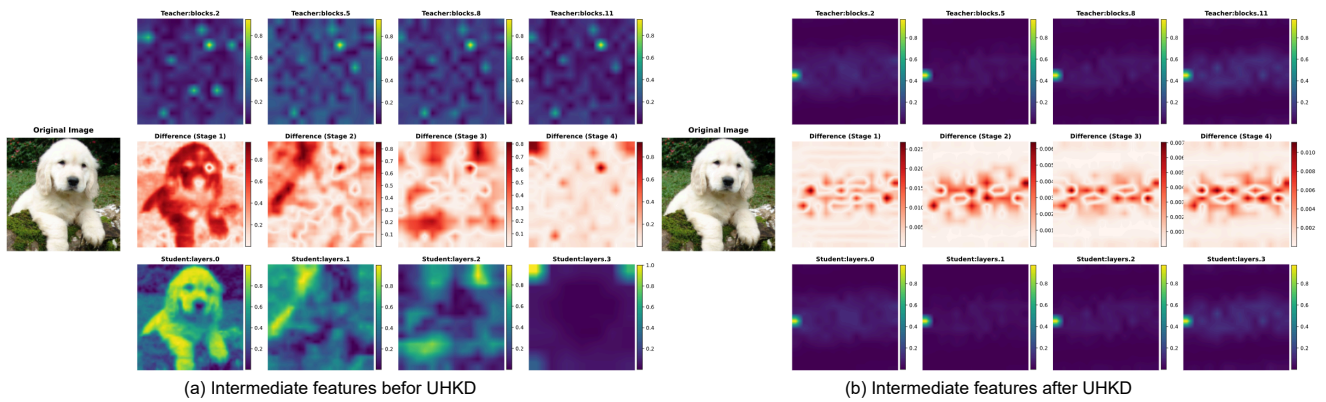


Figure 10. Visualization of intermediate features before and after UHKD. **(a)** Before UHKD; **(b)** After UHKD. In each case, the left column shows the original image, the top and bottom rows show feature maps from different stages of the Mixer-B/16 teacher and Swin-N student, and the middle row shows their difference maps.